Analysis of the Effect of *in situ* Product Removal on the Stability and Performance of a Continuous Bioreactor with Cell Separator for Ethanol Production

Kaushik Ghosh and K. B. Ramachandran*
Department of Biotechnology, Indian Institute of Technology, Madras, Chennai 600036, India

Original scientific paper
Received: September 12, 2006
Accepted: March 1, 2007

In this study, the behaviour of a continuous membrane bioreactor with *in situ* removal of product ethanol by pervaporation and cell recycle has been investigated. The kinetic model used is an unstructured growth model taking into account product as well as substrate inhibition and the product formation rate is represented by the *Leudeking-Piret* model. The effect of pervaporation on the performance of the system with cell separator is evaluated in terms of ethanol productivity and its stability. The stability analysis carried out using elementary principles of bifurcation theory shows that the reactor is characterized by the presence of steady-state multiplicity and hysteresis. The simulation results also demonstrate that the *in situ* removal of ethanol by pervaporation increases productivity as the ethanol inhibition barrier is overcome. Introduction of both pervaporation and cell recycling increases the region of instability in the system but the instability region moves to higher values of dilution rate. This allows stable operation of a fermentor at higher dilution rates to achieve increased productivity.

Key words:
Cell recycling, ethanol fermentation, pervaporation, stability, productivity

Introduction

Because of limited global supply of oil, ethanol has re-emerged as an alternative to, or extender for petroleum-based liquid fuels.[1] Ethanol is obtained from starch plants (grain, mostly corn, maize and tubers like cassava); sugar plants (sugar beet or sugar cane) using biological production technology, which is fermentation and subsequent enrichment by distillation or pervaporation and dehydration. One of the major problems for the efficient and effective production of ethanol from renewable feedstock is the product (ethanol) as well as substrate inhibition of the biocatalyzing micro-organism which results in low productivity.[2]

From the technical viewpoint, one approach to process improvement would be by using a continuous fermentation integrating an ethanol removal operation. This would allow the ethanol concentration in the fermentation broth to be maintained at a level that is minimally inhibitory to fermenting organisms.[3] Continuous ethanol removal from fermentation broths has been accomplished by vacuum distillation[4] gas stripping[5], solvent extraction[6], membrane pervaporation.[7,8] There are many well-developed, stable, highly selective, and permeable membranes available for the continuous removal of ethanol from the fermentation medium[9]. Pervaporation is probably the most promising technique for efficient continuous removal of ethanol from the fermentation broths to minimize ethanol inhibition.[8] It is defined as the transport of liquid through a membrane with simultaneous evaporation of permeates. The development of pervaporation technology began in 1950s. Excellent discussion on pervaporation theory and applications[10,11] and selective permeation of organics including ethanol[12] are available.

It is well known that ethanol yield and productivity can be increased by reducing the effect of ethanol inhibition as well as by maintaining a higher value of yeast cell density in the fermentor. The addition of a cell separator and cell recycling to such a fermentation process may thus lead to better performance and higher productivity.[13]

Using an unsegregated-structured two compartment kinetic model of *Jobses* et al.[14,15] a detailed multiplicity and stability analysis including static/dynamic bifurcation investigation of a continuous membrane fermentor has been carried out by *Grahyan* et al.[16–19] to study the effect of *in situ* ethanol removal on the behaviour of the fermentor. *Garhyan* et al.[20] have also studied the effect of cell recycle in two continuous membrane fermentor configuration for producing ethanol. Effect of introducing cell recycle system on the performance of a continuous recycle hollow fibre plug flow type membrane fermentor has been studied by *Kargupta* et al[21] using modified *Ghose-Tyagi* specific growth

*Corresponding author. E-mail: kbram@iitm.ac.in;
Tel.: +914422574118; Fax: +914422574102

rate model[22] along with *Luedeking-Piret* product formation kinetics.[23]

However, no report has appeared on the performance as well as on the multiplicity and stability analysis of a continuous recycle well mixed membrane bioreactor with continuous *in situ* removal of ethanol by pervaporation using an unstructured nonsegregated growth model.

The system considered in this study has a hypothetical fermentor, which involves the use of a highly ethanol selective membrane, with very high vacuum maintained on the permeate side to increase the driving force and to remove the product away from the membrane surface. The fermentor is also equipped with cell separator to maintain high biomass concentration. This approach has been used to remove inhibitory product (ethanol) *in situ* and to retain high density of biomass in the fermentor.

In this study, specific growth rate model with product and substrate inhibition kinetics[24] which is unstructured as well as unsegregated is used along with *Luedeking-Piret*[23] model for product formation kinetics. The steady state (static) bifurcation behavior of the continuous recycle membrane fermentor separator (CRMFS) system for ethanol production is investigated for a wide range of physically realistic parameters. The multiple steady states for the ethanol fermentation process in a CRMFS are calculated and their stability is determined by following a systematic approach. The effects of different process parameters are also presented. Finally, the performance of CRMFS system as ethanol producer is evaluated and the effects of various process parameters on it are studied.

Bioprocess model

Fig. 1 shows a schematic diagram of the continuous membrane fermentor-separator (CRMFS) with provision for cell separation and recycling. The system consists compartment 1 and 2, separated by a highly ethanol selective membrane. Compartment 1 is the fermentor and compartment 2 is the separator, and the ethanol produced in the fermentor continuously permeates through the membrane. A very high vacuum is maintained in the separator to achieve the partial pressure gradient of ethanol across the membrane. The permeate pressure is always kept low (<5 mm Hg) by a vacuum pump and the permeate ethanol is collected in cold traps. During the process, a purge from the fermentor is used to remove excess medium components such as cells, salts, and byproducts. This type of coupled reactor separator unit has been successfully used in many studies for simultaneous reaction and *in situ* removal of product by pervaporation.[25]

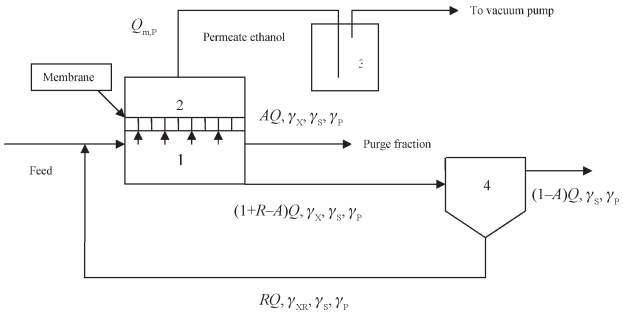

F i g . 1 – *Schematic diagram of a continuous recycle well mixed membrane bioreactor with cell separator: (1) Fermentor; (2) Separator; (3) Cold trap; (4) Settler (Cell separator)*

Assumptions

In developing the mathematical model, the following assumptions have been made:

1. The liquid phase in fermentor and vapour phase in separator are well mixed.

2. Densities of various streams and the volume of the fermentor are considered constant.

3. The bioreactor runs under isothermal condition.

4. Growth and metabolism are assumed not inhibited owing to nutrient limitation or cell crowding.

5. In the separator, very high vacuum is maintained, so that in any axial position the mass transfer resistance in the vapour phase as well as the vapour phase concentration of ethanol may be assumed negligible.

6. The membrane used is highly selective to ethanol and the permeation of the other species and water is negligible.

7. The permeability of the membrane is almost constant within the operating range of the concentration of ethanol in the fermentor.

8. Death and lysis of cells are neglected and the entire biomass is postulated to exhibit a metabolic activity of the same level.

9. Ideal conditions are assumed to prevail in the settler.

10. No loss in viability of cells occurs owing to recycling.

11. The feed is sterile and does not contain any product.

Mass balance equations

The mass balance equations for the proposed CRMFS system can now be expressed by the following equations:

Cell mass balance:

$$\frac{d\gamma_X}{dt} = (\mu - AD)\gamma_X \qquad (1)$$

Substrate balance:

$$\frac{d\gamma_S}{dt} = D_0\gamma_S - \nu\gamma_X - D\gamma_S \quad (2)$$

where, $D_0 = \frac{Q_f}{V}$ and $D = \frac{Q}{V}$.

Product balance:

$$\frac{d\gamma_P}{dt} = -D\gamma_P - \frac{Q_{m,P}}{V} + q\gamma_X \quad (3)$$

Overall mass balance:

$$D_0 = \frac{Q_{m,P}}{\rho V} + D \quad (4)$$

$$Q_{m,P} = \frac{(M_E P_{m,E} A_m)(P_E^0 x_E - y_E P_{sep})}{\delta} \quad (5)$$

Based on assumption 5 and 6, we can write $P_{sep} \approx 0$ and $P_E^0 x_E >> y_E P_{sep}$. Now the equation may be expressed as,

$$Q_{m,p} = \frac{(M_E P_{m,E} A_m P_E^0 x_E}{\delta} \quad (6)$$

For constant value of permeability of ethanol through the membrane (assumption-7), we can define the pervaporation factor as:

$$PF = \frac{M_E P_{m,E} A_m P_E^0}{\delta V \rho_E} \quad (7)$$

PF (h^{-1}) is proportional to the rate of permeation and inversely proportional to the volume of the fermentor. Clearly, for the CRMFS system in which there is no continuous *in situ* ethanol removal $PF = 0$. For calculation of PF, the permeability $P_{m,E}$ can easily be obtained from experimental data for ethanol-water system. The vapour pressure of ethanol can be calculated using the Antoinie equation.

Substitution of eq. (7) in to eq. (6) gives,

$$Q_{m,P} = (PF)V\gamma_P \quad (8)$$

Now substitution of eq. (8) in to eq. (3) and (4) gives,

$$\frac{d\gamma_P}{dt} = -(D + PF)\gamma_P + q\gamma_X \quad (9)$$

and

$$D = D_0 - \frac{(PF)\gamma_P}{\rho} \quad (10)$$

The above set of equations along with the kinetic equations describes the model of the continuous CRMFS system with cell separator and pervaporation.

Kinetic model

To incorporate the product and substrate inhibition effects in the case of ethanol fermentation, various modifications of the *Monod's* equation, as well as other types of equations, have been proposed and summarized by *Dourado* et al.[24] and *Nishiwaki* et al.[26] In this study, the kinetic models used for simulation are the substrate and product inhibited growth model,[24] together with the *Luedeking-Piret*[23] model for product formation. This is an unstructured, nonsegregated model, based on biomass, substrate, and ethanol concentrations.

$$\mu = \frac{\mu_{max} K_P \gamma_S}{(K_P + \gamma_P)\left(K_S + \gamma_S + \frac{\gamma_S^2}{K_i}\right)} \quad (11)$$

$$\nu = \alpha'\mu + \beta' \quad (12)$$

$$q = \alpha\mu + \beta \quad (13)$$

where

$$\alpha' = \frac{\alpha}{Y_{P/S}}$$

and

$$\beta' = \frac{\beta}{Y_{P/S}}$$

The quantities μ_{max}, K_P, K_S, K_i, $Y_{P/S}$, α and β are the model parameters which can be determined experimentally. The numerical values of the model parameters used for the simulations are shown in Table 1. The microbial strain *Sacchromyces cerevisiae* is used to obtain kinetic data. Fermentation conditions are pH 5.0-5.5 and temperature around 30 °C. In order to evaluate the performance of the fermentor as an alcohol producer, ethanol production rate was calculated by the following equation.

Table 1 – *Numerical values of the quantities used in the kinetic model*[23]

Parameter	Value
μ_{max}	0.5 h^{-1}
K_P	4.5 kg m^{-3}
K_S	5.0 kg m^{-3}
K_i	20 kg m^{-3}
ρ	1000 kg m^{-3}
$Y_{P/S}$	0.5 kg kg^{-1}
α	13
β	0.05 h^{-1}

$$P_r = (D + PF)\gamma_P \quad (14)$$

The above equation gives the total ethanol produced in the fermentor. However, the useful product is the pervaporated ethanol which depends on the value of *PF*. Pervaporated ethanol will be close to the ethanol produced by the microbes at values of *PF* much greater than D. Hence, by choosing an appropriate membrane with high *PF*, we can recover all the ethanol as a useful product.

Numerical method

Since the proposed model consists of a set of ordinary differential equations, i.e. a lumped parameter model, it can exhibit a wide range of nonlinear phenomena depending on the values of the model parameters. The model can reach steady state, i.e. point attractor or can exhibit self-sustained oscillations. In this section, methods used to obtain all the steady state values and to determine their stability for the proposed bioreactor model are discussed.

Calculation of steady state values

To determine the steady state values, the accumulation terms (LHS) of the eq. (1), (2) and (9) were set to zero. This gives rise to the following algebraic equations

$$(\mu - AD)\gamma_{X_S} = 0 \quad (15)$$

$$D_0\gamma_{S_f} - D\gamma_S - v\gamma_{X_S} = 0 \quad (16)$$

and

$$-(D + PF)\gamma_{P_S} + q\gamma_{X_S} = 0 \quad (17)$$

where, subscript 's' indicates steady-state value. The three state equations were solved sequentially and/or simultaneously.

Trivial steady state

At trivial steady state $\gamma_{X_S} = 0$, from eq. (16) and (17) it follows that $\gamma_{P_S} = 0$ and $\gamma_{S_S} = \gamma_{S_f}$. This trivial steady state is the "Wash-out" steady state, because no biomass is produced and the substrate concentration in the fermentor is equal to the feed substrate concentration.

Non-trivial steady states

At the non-trivial steady states, balance equation gives

$$(\mu - AD) = 0 \quad (18)$$

Using eq. (10), (11) and (18) γ_{S_S} is expressed in terms of γ_{P_S} as,

$$\gamma_{S_S} = f(\gamma_{P_S}, p) \quad (19)$$

where, the term p represents model operating as well as kinetic quantities.

Similarly, γ_{X_S} can be expressed in terms of γ_{P_S} using eq. (13), (17) and (18) as,

$$\gamma_{X_S} = \frac{(D + PF)\gamma_{P_S}}{(\alpha AD + \beta)} \quad (20)$$

Now substitution of the eq. (19) and (20) in eq. (16) gives a 5th order polynomial equation in γ_{P_S} of the following form.

$$a\gamma_{P_S}^5 + b\gamma_{P_S}^4 + c\gamma_{P_S}^3 + d\gamma_{P_S}^2 + e\gamma_{P_S} + f = 0 \quad (21)$$

where *a, b, c, d, e* and *f* are coefficients which depend on the model kinetic quantities (μ_{max}, K_P, K_S, K_i, $Y_{P/S}$, α, β) and process operating conditions (D_0, A, PF and γ_{S_f} etc.).

The MATLAB function '*roots*' is used to obtain all the 5 roots of eq. (21). Each root corresponds to a non-trivial steady state value of product concentration, γ_{P_S}. The corresponding steady state values of γ_S and γ_X are calculated from eq. (19) and (20) respectively. Mathematical solution is possible for all the 5 non-trivial steady states for this system. All these steady states may not be feasible because of physical constraints. Only the physically feasible steady states are considered for further stability analysis.

Stability analysis of the feasible steady states

Since the calculated steady states were not always stable, it is necessary to check the stability of steady states for making stable fermentor operation.

Linearizing eq. (1), (2) and (9) around a steady state value (γ_{X_S}, γ_{S_S}, γ_{P_S}), the following Jacobian matrix (***J***) was obtained.

$$\boldsymbol{J} = \begin{bmatrix} (\mu_S - AD) & \gamma_{X_S}\mu'_S & \gamma_{X_S}\left(\mu'_P + A\left(\frac{PF}{\rho}\right)\right) \\ -(\alpha'\mu_S + \beta') & -D - (\gamma_{X_S}\mu'_S\alpha') & \gamma_{S_S}\left(\frac{PF}{\rho}\right) - (\gamma_{X_S}\mu'_P\alpha') \\ (\alpha\mu_S + \beta) & (\alpha\mu'_S\gamma_{X_S}) & -\left(D + PF - \left(\frac{PF}{\rho}\right)\gamma_{P_S}\right) + (\gamma_{X_S}\mu'_P\alpha) \end{bmatrix} \quad (22)$$

where

$$\mu'_{S} = \left(\frac{\partial \mu}{\partial \gamma_{S}}\right)_{St.\,st.} = \frac{\mu_{max} K_{P}\left(K_{S} - \frac{\gamma_{S_S}}{K_{i}}\right)}{(K_{P} + \gamma_{P_s})\left(K_{S} + \gamma_{S_S} + \frac{\gamma^{2}_{S_S}}{K_{i}}\right)}$$

$$-\mu'_{P} = \left(\frac{\partial \mu}{\partial \gamma_{P}}\right)_{St.\,st.} = \frac{\mu_{max} K_{P} \gamma_{S_S}}{(K_{P} + \gamma_{P_s})^{2}\left(K_{S} + \gamma_{S_S} + \frac{\gamma^{2}_{S_S}}{K_{i}}\right)}$$

$$D = D_{0} - \frac{(PF)\gamma_{P_S}}{\rho}$$

The stability of each physically feasible steady-state is determined from the eigenvalues of the Jacobian matrix (***J***). For a three-state system, the Jacobian matrix has three eigenvalues. The eigenvalues of the Jacobian matrix (***J***) were determined by using MATLAB function 'eig'.

Criteria for stability

If all the eigenvalues and/or real part of all the complex eigenvalues of the Jacobian matrix are negative, then the corresponding steady state is stable. The multiplicity and stability behaviour of the system are shown in bifurcation diagrams representing the evolution of the steady-state solutions of the model with one or different model parameters. The external dilution rate D_0 is chosen as the bifurcation parameter.

Results and discussions

The steady-state variations of substrate γ_S, product ethanol γ_P and productivity P_r with the external dilution rate D_0 are shown by simulation of the model equations in the one-parameter bifurcation diagrams of Figs 2(a),(b) and (c) for feed condition γ_{S_f} = 100.0 kg m^{-3}, PF = 0.1 h^{-1} and purge fraction A = 0.6. All the bifurcation diagrams show two stable-static branches (solid lines) connected by an unstable static branch (dash lines) in the middle. In Fig. 2(a), the upper branches corresponds to stable low conversion conditions (low biomass concentrations) while high conversion conditions are possible on the lower stable branch. The two stable branches in each figure are connected to the unstable region by a couple of limit (turning) points at external dilution rates respectively D_{LP1} (~0.08 h^{-1}) and D_{LP2} (~0.07h^{-1}). This is due to hysteresis phenomenon. The dynamics of the reactor in this region are determined by start-up conditions. Depending on the initial conditions, the reactor operation may settle on the desired high conversion (lower stable branch in Fig. 2a) or it may move to a low conversion operating point (higher stable branch in Fig. 2a). The phase plane diagram in Fig. 3 shows the dynamic behaviour of the system in this region. It shows in the phase plane diagram that under the same operating conditions (D_0 = 0.075 h^{-1}, PF = 0.1 h^{-1}, A = 0.6 and γ_{S_f} = 100 kg m^{-3}) the system settles into two different steady states (high conversion point attractor, point 2 and low conversion point attractor, point 1) depending on initial start-up conditions. Any abrupt change in the system operating parameters such as dilution rate or

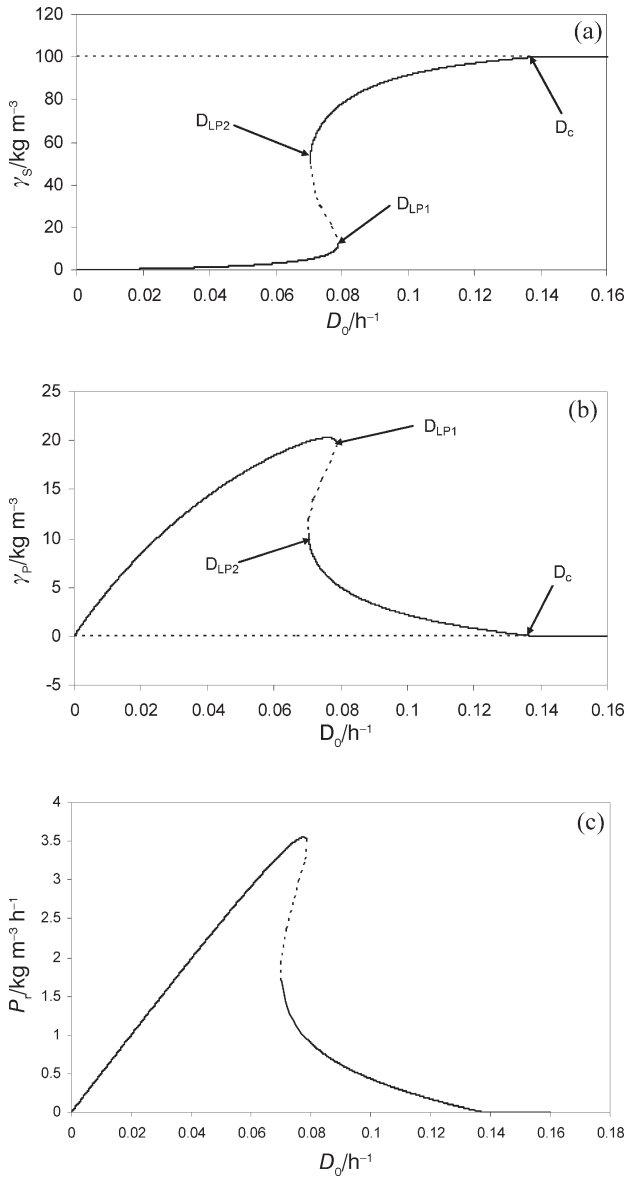

Fig. 2 – *One-parameter bifurcation diagrams. (a) Steady state Substrate concentration γ_S vs. external dilution rate D_0 (b) Steady state Product (ethanol) concentration γ_P vs. external dilution rate D_0. (c) Steady state Productivity P_r vs. external dilution rate D_0 for PF = 0.1 h^{-1} with purge fraction A = 0.6 and γ_{S_f} = 100 kg m^{-3}.* ——— *(stable),* – – – – *(unstable).*

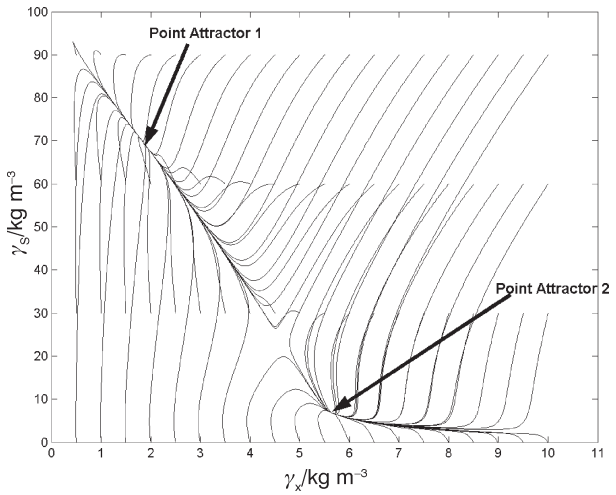

F i g . 3 – *Phase plane diagram, biomass concentration γ_X vs. substrate concentration γ_X showing that under same operating conditions (D_0 = 0.075 h^{-1}, PF = 0.1 h^{-1}, A = 0.6 and γ_{S_f} = 100 kg m^{-3}) the bioreactor settles into two different steady states (point attractor 1 and point attractor 2) depending on the initial start-up conditions*

purge fraction can have irreversible effects on the overall substrate conversion as the system can move from a high conversion (lower branch in Fig. 2a) to a low conversion operating point (higher branch in Fig. 2a). This type of hysteresis effect is not uncommon in continuous fermentation and it has been reported by many researchers.[27,28]

The upper most branch (shown as straight line in Fig. 2a) corresponds to "wash-out" conditions ($\gamma_X = 0$, $\gamma_P = 0$, $\gamma_S = \gamma_{S_f}$). The higher stable branch terminates at the washout branch at a limit point and the corresponding dilution rate is the critical dilution rate (D_C). For external dilution rate $D_{LP1} < D_0 < D_C$, the system has two steady states. The non-washout steady state (higher branch) is stable under these conditions, while the washout steady state is unstable saddle. For external dilution rate $D_0 > D_C$, there is a single steady state, the washout steady state and it is always stable.

Hopf bifurcations can occur in systems with two or more states when two complex eigenvalues cross the imaginary axis, while all other eigenvalues remain negative (stable), as the bifurcation parameter is varied. Therefore, the study of the dynamic bifurcation of the system is not essential to determine whether the system posses any Hopf bifurcation (HB) or not. But if the system posses any Hopf bifurcation (HB), then the dynamic bifurcation studies of the system has to be carried out to explore the actual behaviour of the system around the Hopf bifurcation (HB) point. In this study, the analysis of the nature of the eigenvalues of the Jacobian (***J***) matrix has revealed that there is no Hopf bifurcation (HB) and thus no periodic/ chaotic attractors present in this system. Therefore, the system does not exhibit any oscillatory or chaotic behaviour. Therefore, dynamic bifurcation and the chaotic characteristics of the system have not been investigated.

Effect of operating variables on stability and productivity

In this section, analysis is carried out to study the effect of operating variable on the stability and productivity. Stability analysis can be conveniently seen in a two-parameter bifurcation diagram showing the locus of the two-limit points of hysteresis region that also defines the limits of the instability region. The effect of operating variables on the occurrence of washout conditions are illustrated in this section by showing the locus of the washout limit point.

Effect of feed substrate concentration γ_{S_f} on stability

Fig. 4 shows the effect of feed substrate concentration γ_{S_f} on the hysteresis region for PF = 0 & 0.1 h^{-1} with purge fraction A = 0.6. It can be seen that for each value of substrate concentration γ_{S_f}, two limits points (one on each branch) are expected. These two points correspond to the limits of the region of instability, i.e. hysteresis. It can also be seen that the width of the region and hence the range of instability increases as the feed substrate concentration increases for a given PF. However, with PF = 0, the range of instability doesn't change significantly after a certain value of feed substrate concentration (γ_{S_f} = 300 kg m^{-3}). This is because, with PF = 0 and at high γ_{S_f}, inhibition of growth by both product and substrate becomes significant. Whereas with PF = 0.1 h^{-1} and at high γ_{S_f}, the product inhibition effect gets reduced but the effect

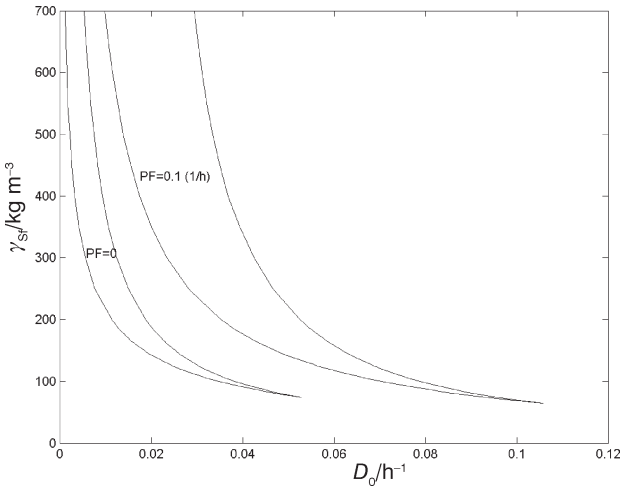

F i g . 4 – *Two-parameter bifurcation diagrams showing the effects of feed substrate concentration γ_{S_f}, on the limits of instability region for different pervaporation factor PF with purge fraction A = 0.6*

of substrate inhibition becomes more significant. Moreover, this instability, i.e. hysteresis region gradually moves towards lower value of external dilution rate with increasing feed substrate concentration. The hysteresis effect is only expected when feed substrate concentration is above ~70 kg m^{-3}, i.e., the point where the two branches collapse. Below this feed substrate concentration no hysteresis is expected and a *Monod*'s type behaviour was only observed. Fig. 5(a)-(b) show an example of this *Monod*'s type behaviour for γ_{S_f} = 40 kg m^{-3} with PF = 0 h^{-1} and A = 0.6. The diagrams show a monotonic behaviour typical of *Monod*'s kinetics.

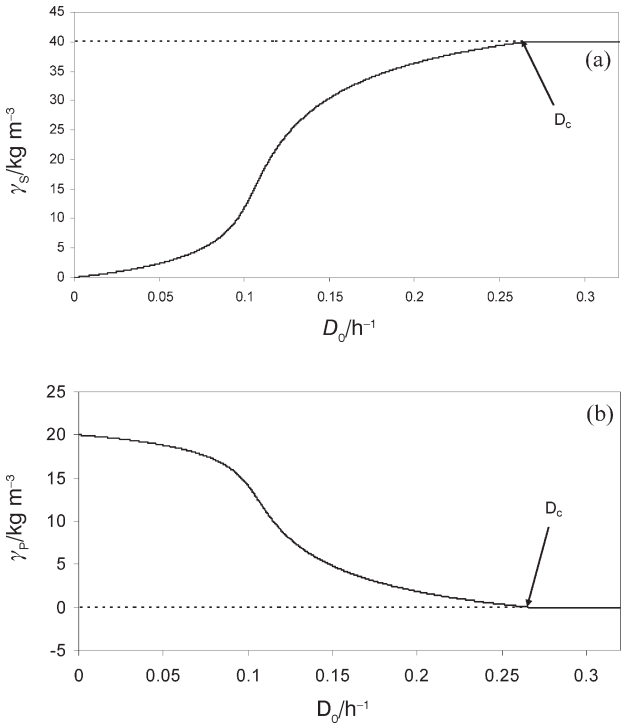

F i g . 5 – *One-parameter bifurcation diagrams showing Monod-like behaviour. (a) Steady state substrate concentration γ_{S_f} vs. external dilution rate D_0 and (b) Product (ethanol) concentration γ_P vs. external dilution rate D_0 for PF = 0 h^{-1} with purge fraction A = 0.6 and γ_{S_f} = 40 kgm^{-3}. ——— (stable), – – – – (unstable)*

Since the growth of the microorganism is inhibited by substrate concentration, an increase in feed substrate γ_{S_f} pushes the washout limit point to lower values of dilution rates. However, for very high value of γ_{S_f} this change is not very significant. This is shown in Fig. 6.

Effect of feed substrate concentration γ_{S_f} on productivity

The effect of the feed substrate concentration, γ_{S_f} on productivity P_r for ethanol fermentation in a CRMFS is shown in Fig. 7 for PF = 0.1 h^{-1} and

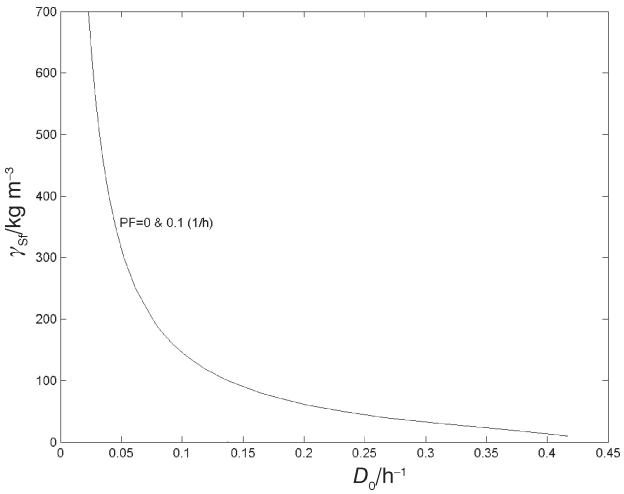

F i g . 6 – *Two-parameter bifurcation diagram showing the effects of feed substrate concentration γ_{S_f} (with PF = 0 h^{-1} and 0.1 h^{-1}) for A = 0.6 on the wash-out conditions*

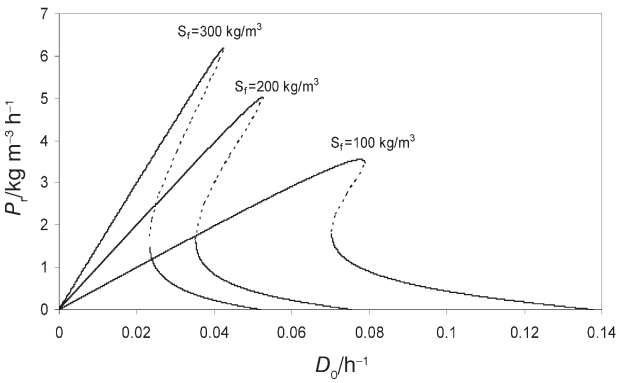

F i g . 7 – *Steady-state productivity P_r vs. external dilution rate D_0, for various values of feed substrate concentrations (γ_{S_f} = 100, 200 and 300 kg m^{-3}) with purge fraction A = 0.6 and PF = 0.1 h^{-1}*

A = 0.6. The figure clearly shows that an increase in feed substrate concentration results in an increase in ethanol productivity because the maximum productivities that can be obtained without introducing instability, i.e. hysteresis into the system are approximately P = 4 kg m^{-3} h^{-1} (at $D_0 \approx 0.025$ h^{-1}), 3.5 kg m^{-3} h^{-1} (at $D_0 \approx 0.035$ h^{-1}) and 3 kg m^{-3} h^{-1} (at $D_0 \approx 0.07$ h^{-1}) with feed substrate concentration γ_{S_f} = 300 kg m^{-3}, 200 kg m^{-3} and 100 kg m^{-3} respectively. But at the same time as the feed substrate concentration increases, width of the instability region increases and also the instability region as the well as washout limit point moves towards lower values of the dilution rate.

Effect of pervaporation factor PF on stability:

Fig. 8 shows the effect of PF on the hysteresis behaviour for different purge fraction (A = 1 & A =

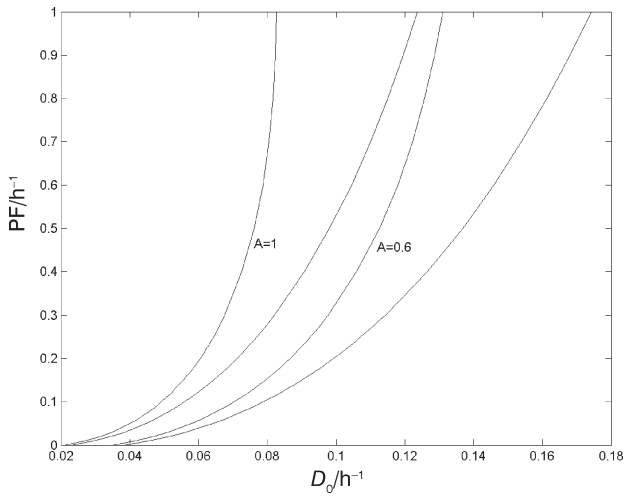

F i g . 8 – *Two-parameter bifurcation diagrams showing the effects of Pervaporation factor PF on the limits of instability region for different purge fraction A with feed substrate mass concentration* γ_{S_f} *= 100 kg m*$^{-3}$

0.6) with feed substrate concentration γ_{S_f} = 100 kg m^{-3}. The figure shows that the width of instability region increases with increase in the values of *PF* and, at the same time, higher *PF* pushes the instability region to higher values of external dilution rate. It also shows that the instability region exist even when *PF* = 0 h^{-1}. Therefore, *in situ* ethanol removal by pervaporation though may increase the width of instability region in the system; it pushes the occurrence of instability in the form hysteresis to a higher range of external dilution rate.

Fig. 9 shows that change in *PF* has no effect on the location of washout limit point. The location of washout limit point is determined by feed substrate concentration (γ_{S_f}) and purge fraction (*A*) and not by Pervaporation factor (*PF*).

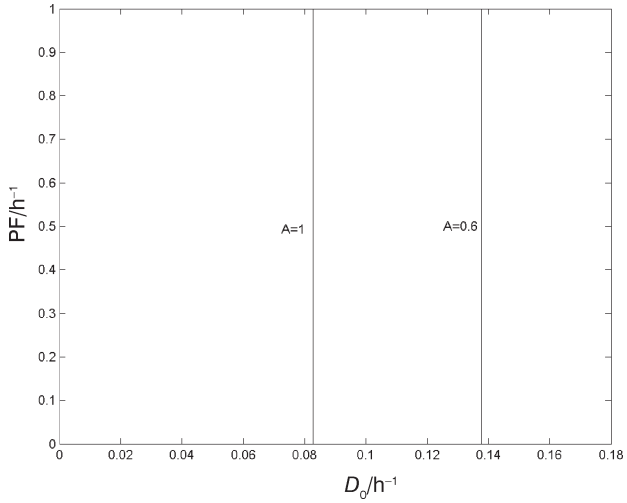

F i g . 9 – *Two-parameter bifurcation diagram showing the effects of pervaporation factor PF with* γ_{S_f} *= 100 kg m*$^{-3}$ *for A = 1 and 0.6 on the wash-out conditions*

Effect of purge fraction A on stability

Figure 10 shows the hysteresis region in the parameter space (*A*, D_0) for two different *PF* (*PF* = 0 & 0.1 h^{-1}), with γ_{S_f} = 100 kg m^{-3}. It can be seen that for each value of the purge fraction *A* (up to the physically realizable value of 1), two limit points (one on each branch) are noted with *PF* = 0 h^{-1} and 0.1 h^{-1}. Although the range of dilution rates exhibiting the hysteresis behaviour increases only slightly as the purge fraction *A* decreases but this range shifts significantly to higher external dilution rates with decrease in the purge fraction *A*, i.e., increase in the cell recycling. The two-parameter bifurcation diagram also predicts a narrow hysteresis region even for the case of no cell recycle, i.e., purge fraction, *A* = 1.

The Fig. 11 shows that an increase in the cell recycle (decrease in purge fraction *A*) pushes the washout limit point to higher values of dilution rates.

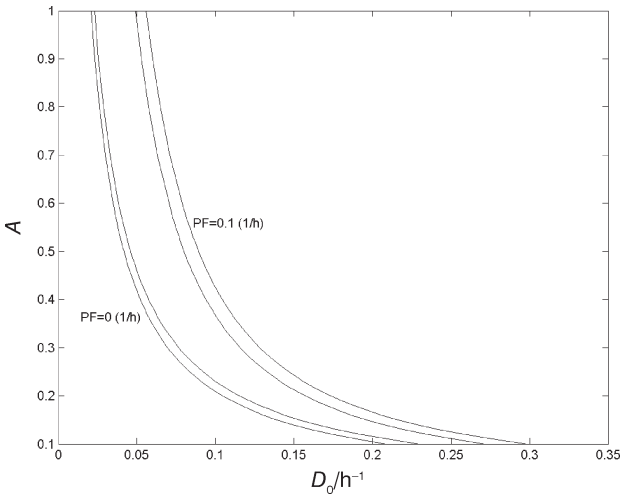

F i g . 1 0 – *Two-parameter bifurcation diagrams showing the effects of purge fraction A on the limits of instability region for different PF with* γ_{S_f} *= 100 kg m*$^{-3}$

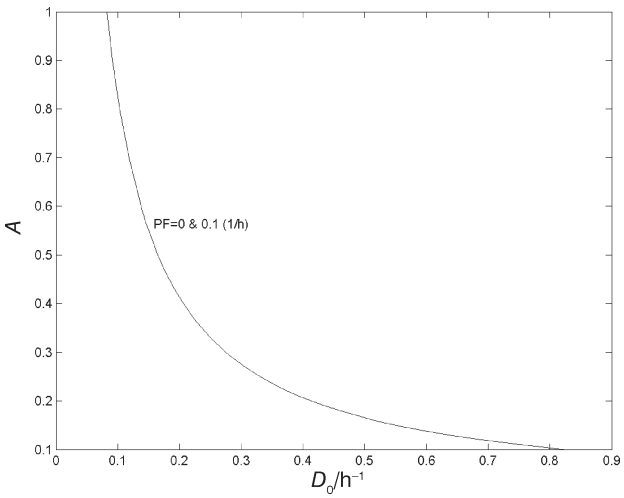

F i g . 1 1 – *Two-parameter bifurcation diagram showing the effects of purge fraction with* γ_{S_f} *= 100 kg m*$^{-3}$ *(with PF = 0 h*$^{-1}$ *and 0.1 h*$^{-1}$*) on the wash-out conditions*

Effect of pervaporation factor PF and purge fraction A on productivity

Fig. 12 shows the effect of the pervaporation factor (*PF*) and purge factor (*A*) on the productivity for a feed substrate concentration, γ_{S_f} = 300 kg m^{-3}. An increase in *PF* not only results in increase in highest productivity that can be achieved with out any instability for a given value of purge fraction *A* but also causes the dilution rate corresponding to this productivity to be increased. It can be seen from the figure that for a process with cell recycling (*A* = 0.6), the value of highest achievable productivity without any hysteresis is higher than that could be obtained without cell recycling (*A* = 1) for a given pervaporation factor, *PF*. It is further observed that the use of cell recycling (*A* = 0.6) increases the highest achievable productivity without instability in the system from ~0.5 kg m^{-3} h^{-1} to ~1 kg m^{-3} h^{-1}, for operation without using pervaporation (*PF* = 0 h^{-1}). However, continuous ethanol permeation with pervaporation (*PF* = 0.1 h^{-1}), results in a considerable improvement in ethanol productivity that can be obtained without instability. Productivity increases from about 3 kg m^{-3} h^{-1} to 4 kg m^{-3} h^{-1} as purge fraction, *A* is reduced from *A* = 1 to *A* = 0.6. The figure also shows that the effect of change in *PF* is much more pronounced for operation with cell recycling compared with that without cell recycling. Furthermore, for the system with cell recycling (*A* = 0.6), cell washout occurs at a higher external dilution rate ($D_0 \approx 0.051$ h^{-1}) compared to ($D_0 \approx 0.03$ h^{-1}) the system without cell recycling (*A*= 1). These results show that by employing a membrane with high *PF* value and using a low purge fraction *A*, the bioreactor can be operated stably even at very high external dilution rate to get high ethanol productivity.

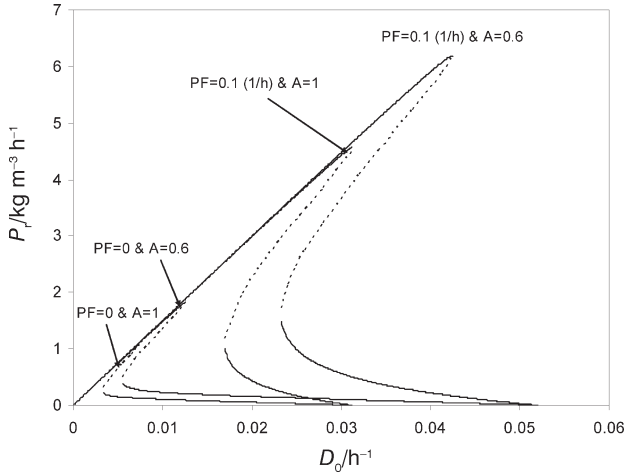

F i g . 1 2 – *Steady-state productivity P_r vs. external dilution rate D_0, for various values of pervaporation factor (PF = 0 and 0.1 h^{-1}) with purge fraction A = 1 (without cell recycling) and A = 0.6 (with cell recycling) and γ_{S_f} = 300 kg m^{-3}*

Effect of model kinetic quantities

In this section, sensitivity analysis of the model kinetic quantities such as product inhibition constant K_p and substrate inhibition constant K_i have been discussed.

Effect of product inhibition constant K_p

Fig. 13 shows the effect of the product inhibition constant K_P on the hysteresis region, with γ_{S_f} = 100 kg m^{-3}, *PF* = 0.1 h^{-1} for purge fraction *A* = 1 & *A* = 0.6. It can be seen that two branches exist even for small positive values of K_P and the width of multiplicity region increases and gets shifted to higher external dilution rate as K_P increases. This is because, with increasing K_p, the effect of product inhibition gets alleviated and only the inhibition of growth due to substrate becomes predominant.

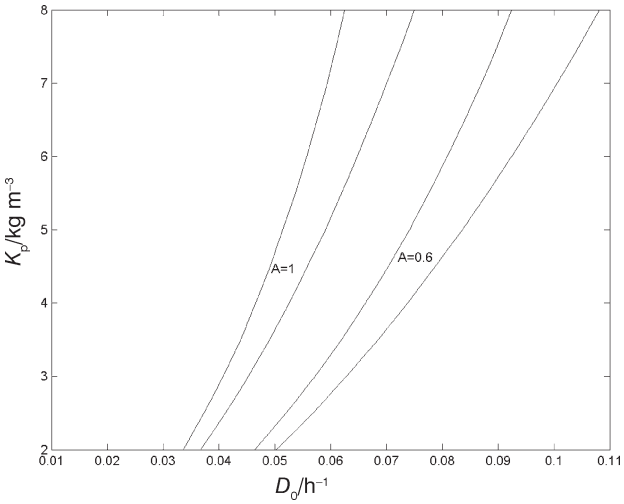

F i g . 1 3 – *Two-parameter bifurcation diagrams showing the effects of product inhibition constant K_P on the limits of instability region for different purge fraction (A = 1 and 0.6) with γ_{S_f} = 100 kg m^{-3} and PF = 0.1 h^{-1}*

The effect of K_p on washout limit point is shown in the Fig. 14. This shows that K_p has no effect on washout dilution rate.

Effect of substrate inhibition constant K_i

Fig. 15 shows the effect of the substrate inhibition constant K_i on the hysteresis region, with γ_{S_f} = 100 kg m^{-3}, purge fraction *A* = 0.6 and for PF = 0 & 0.1 h^{-1}. The figure shows that that the width of multiplicity region decreases and gets shifted to higher external dilution rate as K_i increases and eventually at high value of K_i, the two branches collapse. Therefore, the system does not exhibit any hysteresis behaviour when K_i > 31 kg m^{-3} and K_i > 35 kg m^{-3}, for PF = 0 & 0.1 h^{-1} respectively. This shows that hysteresis behaviour is mainly due to inhibition of

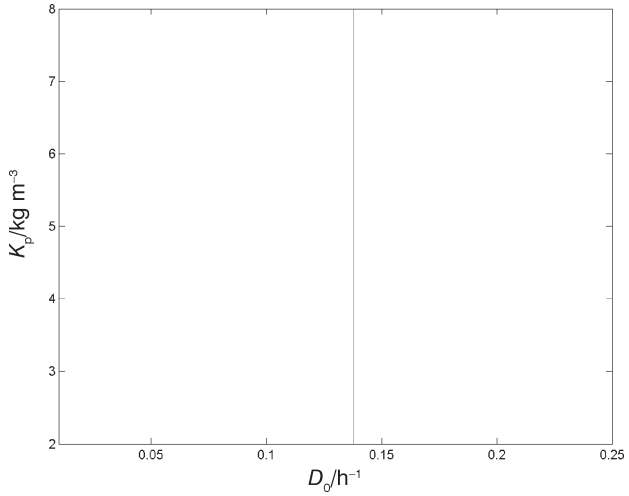

F i g . 1 4 – *Two-parameter bifurcation diagram showing the effects of product inhibition constant K_P with γ_{S_f} = 100 kg m^{-3}, PF = 0 h^{-1} and A = 0.6 on the washout conditions*

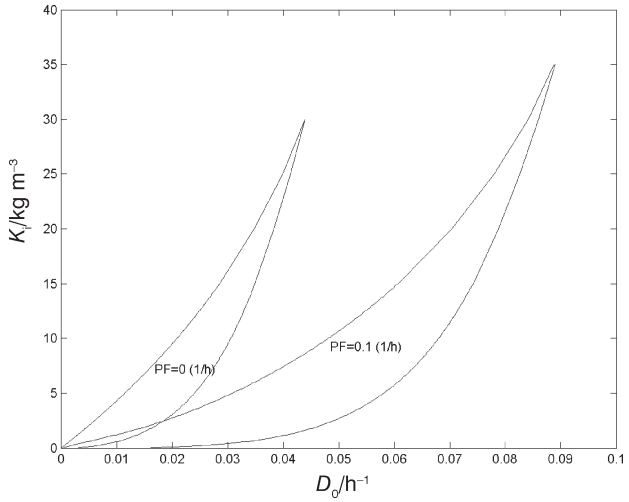

F i g . 1 5 – *Two-parameter bifurcation diagrams showing the effects of substrate inhibition constant K_i on the limits of instability region for PF = 0 h^{-1} and 0.1 h^{-1} with γ_{S_f} = 100 kg m^{-3} and A = 0.6*

growth by the substrate, because at higher values of K_i the substrate inhibition effect gets reduced and attenuation of product inhibition effect by pervaporation not only widens the multiplicity region but also pushes it to higher values of external dilution rate.

As expected, an increase in K_i, i.e. decrease in substrate inhibition effect, pushes the washout limit point to higher values of dilution rates. This is shown in Fig. 16.

Comparison of results with other studies

The stability analysis shows that the model does not exhibit any Hopf bifurcation and *in situ* ethanol removal by pervaporation increases instability of the system. This is contradictory to the earlier work of *Garhyan* et al.[16,17,18], where the system posses Hopf

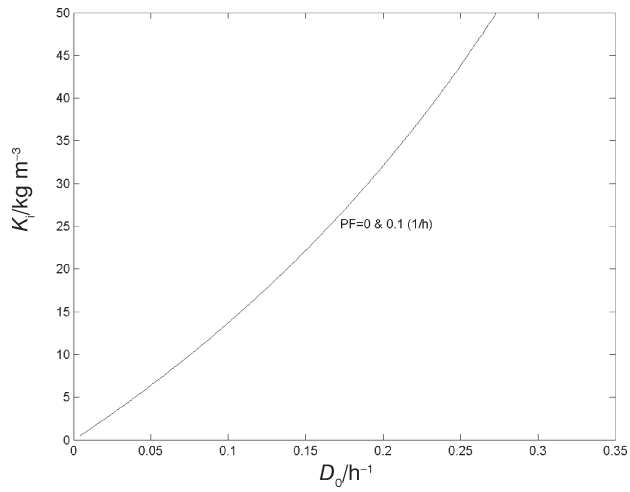

F i g . 1 6 – *Two-parameter bifurcation diagram showing the effects of substrate inhibition constant K_i with γ_{S_f} = 100 kg m^{-3}, PF = 0 h^{-1} and A = 0.6 on the wash-out conditions*

bifurcation and ethanol removal tends to stabilize the system. This is because the kinetic model used by them is quite different from the kinetic model used in this study. *Garhyan* et al.[16–20] used the kinetic model of *Jobes* et al. which is structured and non-segregated one. It can be shown that the kinetic model used by *Garhyan* et al[16–20] can not properly represent inhibitory effect of product ethanol on the growth of micro-organism. In their case even at high product (ethanol) concentration, the fraction of active biomass ($Y_{E/X} = \gamma_E/\gamma_X$) was much larger than unity and the specific growth rate μ of *Zymomonas mobilis* becomes much higher than maximum specific growth rate, μ_{max}. As a result, "wash-out" of biomass does not occur in the continuous fermentor even when the fermentor is operated at a dilution rate, which is much higher than maximum specific growth rate (μ_{max} = 1). This can be seen in Fig. 12 of Ref. 19 where biomass wash-out is not achieved at dilution rate which is as high as 2.5 h^{-1} (> μ_{max}). From the continuous fermentor operation point of view, this is very strange and unusual. A simple unstructured and non-segregated kinetic model used in this study can properly represent the inhibitory effect of both product (ethanol) and substrate on the growth of microorganism.

Conclusion

In the present work, the behaviour of an unstructured model of a continuous, membrane fermentor with *in situ* removal of product ethanol by pervaporation, cell recycle and with substrate-product inhibition kinetics has been investigated. A detailed static (steady state) bifurcation analysis of the system has been performed and stability analysis of multiple steady states have been

presented. The stability analysis shows that the model exhibits rich stability characteristics ranging from simple *Monod*-like behaviour to hysteresis behaviour. However, the model does not exhibit Hopf bifurcation and periodic attractors.

The investigation also shows that high feed substrate concentrations give high productivity but the system is characterized by the presence of hysteresis behaviour, where a high conversion stable static branch coexists with a low conversion one over some range of external dilution rate. However, shifting of this hysteresis behaviour to a higher value of dilution rate is possible by continuous *in situ* removal of ethanol by pervaporation through an ethanol selective membrane and consequently higher productivities can be obtained.

Elimination of cell washout allows the continuous fermentor with cell separator unit to be operated at a very high dilution rate, i.e., it reduces the required fermentor volume for the attainment of the same value of productivity. It also helps in further shifting the instability region to higher a value of dilution rate. However, the range of instability, i.e. hysteresis region increases with both pervaporation and cell recycling (decreasing purge fraction, A). Though introduction of pervaporation and cell recycling cannot completely eliminate the instability in this system, they push the hysteresis region to a higher value of dilution rate and improves the productivity of a given fermentor system.

Nomenclature

A – purge fraction
A_m – cross sectional area of the separator, m^2
D – Internal dilution rate based on effluent flow rate, h^{-1}
D_0 – external dilution rate based on feed flow rate, h^{-1}
D_c – washout external dilution rate, h^{-1}
Q – effluent flow rate from the fermentor, $m^3\ h^{-1}$
$Q_{m,p}$ – permeate ethanol mass flow rate, kg h^{-1}
Q_f – feed flow rate, $m^3\ h^{-1}$
$\boldsymbol{J}$ – Jacobian matrix
K_P – product (ethanol) inhibition constant for growth, kg m^{-3}
K_S – Monod saturation constant for growth, kg m^{-3}
K_i – substrate inhibition constant for growth, kg m^{-3}
M_E – molar mass of ethanol, kg $kmol^{-1}$
γ_P – product concentration in fermentor, kg m^{-3}
P_E^0 – vapour pressure of pure ethanol, kPa
PF – pervaporation factor, h^{-1}
γ_{P_f} – product concentration in feed, kg m^{-3}
P_{sep} – pressure in separator, kPa
γ_{P_S} – product concentration in fermentor at steady state, kg m^{-3}
P_r – productivity of ethanol at steady state, kg $m^{-3}\ h^{-1}$
q – specific product (ethanol) formation rate, h^{-1}
$P_{m,E}$ – permeability of ethanol through the membrane (kmol $m^{-1}\ h^{-1}\ kPa^{-1}$
R – recycle ratio (volumetric)
γ_S – substrate concentration in the fermentor, kg m^{-3}
γ_{S_f} – substrate concentration in the feed, kg m^{-3}
γ_{S_S} – substrate concentration in the fermentor at steady state, kg m^{-3}
t_m – thickness of the membrane, m
V – volume of the fermentor, m^3
γ_X – biomass concentration in fermentor, kg m^{-3}
γ_{X_f} – biomass concentration in feed, kg m^{-3}
γ_{X_R} – biomass concentration in recycle feed, kg m^{-3}
γ_{X_S} – biomass concentration in fermentor at steady state, kg m^{-3}
γ_E – concentration of the key internal component, kg m^{-3}
x_E – mole fraction of ethanol in the liquid phase (fermentor)
y_E – mole fraction of ethanol in the vapour phase (permeate)
$Y_{P/S}$ – yield of ethanol based on substrate consumed, kg kg^{-1}
$Y_{E/X}$ – mass fraction of active components, kg kg^{-1}
α – constant used in Luedeking-Piret model
β – constant used in Luedeking-Piret model, h^{-1}
μ – specific cell growth rate, h^{-1}
μ_{max} – maximum specific growth rate, h^{-1}
υ – specific substrate consumption rate, h^{-1}
ρ – density of the fermentation broth, kg m^{-3}
ρ_E – density of ethanol, kg m^{-3}

Abbreviations

CRMFS – Continuous Recycle Membrane Fermentor Separator
PF – Pervaporation Factor, h^{-1}

References

1. *Ward, O. P., Singh, A.,* Adv. Appl. Microbiol. **51** (2002) 53.
2. *Luong, J. H. T.,* Biotechnol. Bioeng. **27** (1985) 280.
3. *Naser, S. F., Fournier, R. L.,* Biotechnol. Bioeng. **32** (1988) 628.
4. *Ramalingham, A., Finn, R. K.,* Biotechnol. Bioeng. **19** (1977) 583.
5. *Fournier, R. L.,* Biotechnol. Bioeng. **31** (1988) 235.
6. *Miner, M., Goma, G.,* Biotechnol. Bioeng. **24** (1982) 1565.
7. *Nakoa, S. I., Saitoh, F., Asakura, T., Toda, K., Kimura, S.,* J. Membrane Sci. **30** (1987) 273.
8. *Cho, C. W., Hwang, S. T.,* J. Membrane Sci. **10** (1982) 253.
9. *O'Brien, D. J., Craig, Jr., J. C.,* Appl. Microbiol. Biotechnol. **44** (1996) 699.
10. *Belafi-Bako, K., Kabiri-Badr, A., Dormo, N., Gubicza, L.,* Hung. J. Ind. Chem. **28** (2000) 175.

11. *Wynn, N.,* Chem. Eng. Prog. **97** (2001) 66.
12. *Hagg, M. B.,* Sep. Purif. Methods **27** (1998) 51.
13. *Hamer, G.,* Biotechnol. Bioeng. **24** (1982) 511.
14. *Jobses, I. M. L., Egberts, G. T. C Ballen, A. V., Roels, J. A.,* Biotechnol. Bioeng. **27** (1985) 984.
15. *Jobses, I. M. L., Egberts, G. T. C., Luyben, K. C. A. M., Roels, J. A.,* Biotechnol. Bioeng. **28** (1986) 868.
16. *Mahecha-Botero, A., Garhyan, P., Elnashaie, S. S. E. H.,* Nonlinear Analysis: Real World Applications. **7** (2006) 432.
17. *Mahecha-Botero, A., Garhyan, P., Elnashaie, S. S. E. H.,* Mathematical and Computer Modelling. **41** (2005) 391.
18. *Garhyan, P., Elnashaie, S. S. E. H.,* Mathematical and Computer Modelling **39** (2004) 381.
19. *Garhyan, P., Elnashaie, S. S. E. H., Al-Haddad, S. M., Ibrahim, G., Elshishini, S. S.,* Chem. Eng. Sci. **58** (2003) 1479.
20. *Garhyan, P., Elnashaie, S. S. E. H.,* Chem. Eng. Sci. **59** (2004) 3235.
21. *Kargupta, K., Datta, S., Sanyal, S. K.,* Biochemical Engineering Journal **1** (1998) 31.
22. *Ghose, T. K., Tyagi, R. D.,* Biotechnol. Bioeng. **21** (1979) 1387.
23. *Luedeking, R., Piret, E. L.,* J. Biochem. Microbiol. Technol. Eng. **1** (1959) 393.
24. *Dourado, A., Goma, G., Albuquerque, U., Sevely, Y.,* Biotechnology and Bioengineering **29** (1987) 187.
25. *Won, K., Hong, J., Kim, K., Moon, S. W.,* Process Biochemistry **41** (2006) 264.
26. *Nishiwaki, A., Dunn, I. J.,* Biochemical Engineering Journal **4** (1999) 37.
27. *Ajbar A.,* Wat. Res. **35** (2001) 1201.
28. *Ajbar, A., Alumaizi, K.,* Math. Comput. Modelling. **31** (2000) 159.